IMAGE DENOISING USING OPTIMAL COLOR SPACE PROJECTION

Nai-Xiang Lian, Vitali Zagorodnov, and Yap-Peng Tan

School of Electrical and Electronic Engineering
Nanyang Technological University, Singapore

ABSTRACT

Denoising of color images can be improved by exploiting strong correlation between high-frequency content of different color components. We show that for typical color images high correlation also means similarity, and propose to exploit this property using an optimal luminance/color-difference space projection. Experimental results confirm that denoising in the proposed color space yields superior performance, both in PSNR and visual quality sense, compared to that of existing solutions.

1. INTRODUCTION

In the last decade, wavelet transform has gained popularity in image denoising due to its good edge-preserving properties. However, most existing wavelet-based denoising techniques [1]-[4] assume the image to be grayscale. Grayscale image denoising can be straightforwardly extended to color images by applying it to each color component independently. However, better denoising should exploit strong inter-color correlations present in typical color images. For example, Pižurica and Philips [5] updated local activity parameter of their grayscale image denoiser with the average value of the wavelet coefficients at the same image location. Scheunders and Driesen [6] treated wavelet coefficients of color components as a signal vector. Estimated covariance matrix of this vector was used to derive the linear minimum mean squared error (LMMSE) estimate by taking into account the inter-color correlations.

Other researchers have proposed to exploit the inter-color correlations by transforming images into a suitable color space. For example, Ben-Shahar [7] used Hue-Saturation-Value (HSV) color space. Chan *et al.* [8] have found that the chromaticity-brightness (CB) decomposition, another color space transformation, can lead to better restored images than denoising in RGB or HSV space. It is easy to show that appropriate color transformation (or projection) can improve the denoising performance. For example, using YCbCr space [9] improves the performance by up to 1.3 dB compared to denoising in RGB space; see Table 3. However, YCbCr space is not necessarily optimal for image denoising.

In this paper we propose an optimal color space projection that is adapted to image data and yields superior to existing solutions in denoising performance. The projection is derived based on a *key observation* that high-frequency wavelet coefficients across image color components are strongly correlated and similar. Even though the correlation of color components is a well known property, a particularly strong (close to 1) correlation between *high-frequency* content of color components has only recently been discovered [11, 12]. This property has since been successfully applied to color filter array (CFA) demosaicking [11]-[13] and implicitly to color image denoising [6, 5]. Our work goes a step further and shows that in a typical color image the high frequency contents across color components are not only highly correlated but also *similar*.

Table 1. Pairwise correlation of wavelet coefficients in the three finest scales.

Color Image	Scale	R & G LH	R & G HL	R & G HH	G & B LH	G & B HL	G & B HH
1	1	0.983	0.993	0.995	0.991	0.996	0.994
	2	0.978	0.991	0.997	0.992	0.997	0.997
	3	0.947	0.968	0.989	0.995	0.995	0.995
2	1	0.811	0.879	0.969	0.979	0.989	0.980
	2	0.687	0.834	0.974	0.973	0.985	0.992
	3	0.256	0.584	0.857	0.958	0.957	0.985
3	1	0.942	0.964	0.957	0.887	0.950	0.939
	2	0.951	0.960	0.974	0.877	0.929	0.962
	3	0.917	0.893	0.913	0.767	0.741	0.826

As we intend to show, similarity of detail wavelet coefficients explains the performance gain when denoising in luminance/color-difference images. The luminance Y is an additive combination of R, G and B color components and hence preserves the high-frequency image content. On the other hand, the color differences Cb and Cr are obtained by subtracting the color components: Cb $\propto$ Y-B and Cr $\propto$ Y-R. This effectively cancels out high frequencies, leading to smoother images, which are easier to denoise.

Building on these observations, we derive an optimal luminance/color-difference space projection that minimizes the noise variance in the luminance image, leading to better edge preservation. Color-difference images comprise a larger portion of noise but are smooth and hence can be efficiently denoised without sacrificing the quality.

2. INTER-COLOR CORRELATIONS OF HIGH-FREQUENCY COEFFICIENTS

Gunturk *et al.* [11] have shown that high-frequency wavelet coefficients of color components are strongly correlated, with correlation coefficients ranging from 0.98 to 1 for most images. This property has been widely exploited in color filter array (CFA) demosaicking [11]-[13]. We replicated Gunturk *et al.*'s [11] results for Daubechies-4 wavelet[1] and the three finest scales in Table 1. These results demonstrate that correlations remain strong even for coarser scales. Here LH, HL and HH are vertical, horizontal and diagonal detail wavelet subbands, respectively. Overall, HH subband correlations are the strongest among all the subbands.

In general, perfect correlation between two random variables does not necessarily mean their equality. However, this is the case for high-frequency coefficients of color components, as follows from the 3D scatter diagrams of high-frequency wavelet coefficients in Fig. 1. Here, the coordinates of each point are the magnitudes of the R, G, and B detail wavelet coefficients taken from the same image

[1] Its mother wavelet filter is $(0.4830, 0.8365, 0.2241, -0.1294)$.

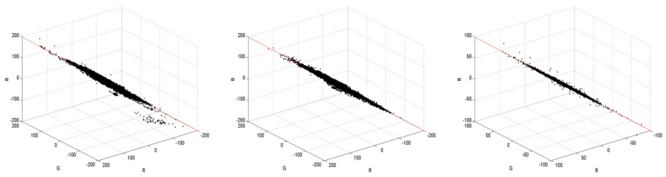

(a) LH (b) HL (c) HH

Fig. 1. Scatter plots of detail wavelet coefficients. The coordinates of each point are the values of the R, G, and B components.

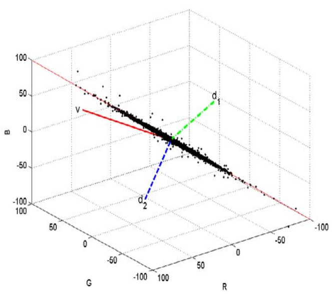

Fig. 2. Basis vectors of YCbCr space projection.

location (first image in Fig. 3). The points are compactly clustered along the line of vector $\mathbf{1} = (1, 1, 1)^T$. Similar scatter diagrams can be obtained for all other test images. These results are similar to Hel-Or's directional derivatives scatter plots [12], but include all detail wavelet coefficients.

The scatter plots also suggest that there exists a more efficient basis capable of compact representation of the wavelet coefficients. This decorrelation property has been extensively employed in color image compression, by transforming the image from RGB to YCbCr space [9]. Let RGB space correspond to the standard basis in 3D, then the basis vectors for a typical YCbCr space are $\boldsymbol{v} = (0.299, 0.587, 0.114)^T$, $\boldsymbol{d}_1 = (-0.147, -0.289, 0.436)^T$ and $\boldsymbol{d}_2 = (0.615, -0.515, -0.100)^T$ [9]. Let x_1, x_2 and x_3 be the values of the R, G and B detail wavelet coefficients (in the horizontal, vertical, or diagonal subband) of a particular image location, respectively. We call $\boldsymbol{x} = (x_1, x_2, x_3)^T$ a signal vector. In Figure 2 we overlay the basis vectors of YCbCr space on the scatter plot of all signal vectors. As we can see, vectors $\boldsymbol{d}_1$ and $\boldsymbol{d}_2$ are orthogonal to vector $\mathbf{1}$. Hence, the projection of the signal vectors onto $\boldsymbol{d}_1$ and $\boldsymbol{d}_2$ is close to zero. This leads to cancelation of high frequencies and smoother color-difference images that are easier to compress and denoise.

Fig. 2 also shows that vector $\boldsymbol{v}$ is not aligned with vector $\mathbf{1}$. The reason is that the so defined luminance Y approximates the grayscale image intensity and is backward compatible with the older black-and-white analog television sets [9]. However, there is a large family of luminance/color-difference spaces, all having basis vectors $\boldsymbol{d}_1$ and $\boldsymbol{d}_2$ orthogonal to $\mathbf{1}$, but using different definitions of Y, i.e. orthonormal double-opponent color-difference basis [10] where vector $\boldsymbol{v}$ aligned with $\mathbf{1}$. In Section 3 we show that an optimal color space for image denoising should be adapted to image noise statistics.

Table 2. PSNR performance (in dB) of Y, Cb and Cr using the uHMT method. For uniform noise, the noise standard deviations added to {R, G, B} are equal to $\sigma_n = \{0.1, 0.1, 0.1\}$; for nonuniform noise, $\sigma_n = \{0.15, 0.10, 0.05\}$. These two types of noise remain the same for all other experiments in the paper.

Color	Uniform noise			Nonuniform noise		
Image	Y	Cb	Cr	Y	Cb	Cr
1	26.69	37.46	36.68	26.16	38.39	35.69
2	30.96	36.90	35.56	30.59	37.99	34.55
3	30.96	36.43	36.96	30.47	37.81	36.09
4	30.73	37.69	36.14	30.37	38.85	35.16
5	26.80	35.85	36.06	26.18	36.78	35.08
6	27.57	35.99	36.65	26.95	36.15	35.11

3. THE OPTIMAL COLOR SPACE PROJECTION

For the sake of simplicity, we assume perfect correlation, namely

$$E(x_i x_j) = \sqrt{E(x_i^2)E(x_j^2)} = \sqrt{s_i^2 s_j^2},\ \forall i, j \tag{1}$$

where x_i's are the detail wavelet coefficients in the i-th color component of the noiseless image, and $s_i^2 \equiv E(x_i^2)$. For a typical color image we have $s_1^2 \simeq s_2^2 \simeq s_3^2 = \bar{s}^2$ (see discussion in Section 2). However, the results derived in this section are applicable to arbitrary signal variances.

Let vector $\boldsymbol{s} = (s_1, s_2, s_3)^T$. We consider a family of luminance/color-difference spaces with basis vectors $(\boldsymbol{v}, \boldsymbol{d}_1, \boldsymbol{d}_2)$, where $\boldsymbol{d}_1$ and $\boldsymbol{d}_2$ are orthogonal to $\boldsymbol{s}$. Let $x_v = \boldsymbol{v}^T\boldsymbol{x}$ be the luminance projection, and $x_{d_i} = \boldsymbol{d}_i^T\boldsymbol{x}, i = 1, 2$, be the color-difference projections. Varying the direction of $\boldsymbol{d}_i$ changes the noise components of x_{d_i} only; the signal component of x_{d_i} remains small. This leads to good denoising performance. On the other hand, the luminance x_v has a large signal component. Its denoising performance can be improved by reducing the projected noise variance.

This observation is illustrated in Table 2, where we apply a popular uHMT denoising approach [2] to color components in YCbCr space. Denoising Cb and Cr leads to 6-7 dB better PSNR than denoising Y. Hence, the performance of luminance denoising, and not that of the color differences, is the key factor in the overall denoising performance.

Note that the basis vectors are not orthogonal to each other in general, because $\boldsymbol{d}_1$ and $\boldsymbol{d}_2$ can not be simultaneously orthogonal to $\boldsymbol{v}$ and $\boldsymbol{s}$. To simplify the analysis we normalize the coordinates of $\boldsymbol{v} = (v_1, v_2, v_3)^T$ so that the variance of the signal projection onto $\boldsymbol{v}$ is fixed. This is the topic of the following lemma.

Lemma 1 *Let $\boldsymbol{x}$ be a random vector that satisfies assumption (1). If we normalize $\boldsymbol{v}$ so that $\boldsymbol{v}^T\boldsymbol{s} = 1$, then the expected squared norm of the projection of $\boldsymbol{x}$ onto $\boldsymbol{v}$ is always equal to 1 and hence doesn't depend on $\boldsymbol{v}$.*

Proof: Let $x_v = \boldsymbol{v}^T\boldsymbol{x}$. Then $E(x_v^2) = E(\boldsymbol{v}^T\boldsymbol{x}\boldsymbol{x}^T\boldsymbol{v}) = \boldsymbol{v}^T E(\boldsymbol{x}\boldsymbol{x}^T)\boldsymbol{v} = \boldsymbol{v}^T\boldsymbol{s}\boldsymbol{s}^T\boldsymbol{v} = 1$. ■

If the variance of x_v is fixed, then choosing the direction of vector $\boldsymbol{v}$ that minimizes the noise projection will minimize the estimation error of the luminance. In general, this doesn't guarantee the optimality of $\boldsymbol{v}$, since the contribution of the luminance component in the inverse formula might depend on $\boldsymbol{v}$. However, Lemma 2 shows that the constraint $\boldsymbol{v}^T\boldsymbol{s} = 1$ also fixes the contribution of x_v in the inverse projection.

Lemma 2 *Let $\boldsymbol{x} = (x_1, x_2, x_3)^T$ be a random vector that satisfies assumption (1). Let $\mathbf{T}$ be an invertible color projection, such that*

$$\begin{pmatrix} x_v \\ x_{d_1} \\ x_{d_2} \end{pmatrix} = \mathbf{T} \begin{pmatrix} x_1 \\ x_2 \\ x_3 \end{pmatrix} = \begin{pmatrix} \boldsymbol{v}^T \\ \boldsymbol{d}_1^T \\ \boldsymbol{d}_2^T \end{pmatrix} \begin{pmatrix} x_1 \\ x_2 \\ x_3 \end{pmatrix} \tag{2}$$

where $\boldsymbol{v}^T\boldsymbol{s} = 1$ and $\boldsymbol{d}_1^T\boldsymbol{s} = \boldsymbol{d}_2^T\boldsymbol{s} = 0$. Then, the corresponding inverse projection is

$$\begin{pmatrix} x_1 \\ x_2 \\ x_3 \end{pmatrix} = \begin{pmatrix} s_1 \\ s_2 \\ s_3 \end{pmatrix} x_v + \mathbf{R} \begin{pmatrix} x_{d_1} \\ x_{d_2} \end{pmatrix} \tag{3}$$

where $\mathbf{R}$ is a 3×2 matrix.

Proof: Let $\mathbf{T}^{-1} = (\boldsymbol{r}, \mathbf{R})$, where $\boldsymbol{r}$ is the first column of $\mathbf{T}^{-1}$. From $\mathbf{T}\mathbf{T}^{-1} = \mathbf{I}$ it follows that $\boldsymbol{v}^T\boldsymbol{r} = 1$ and $\boldsymbol{d}_1^T\boldsymbol{r} = \boldsymbol{d}_2^T\boldsymbol{r} = 0$. Hence, clearly $\boldsymbol{r} = \boldsymbol{s}$ and we obtain (3). ■

To simplify the inverse projection, we use four basis vectors (one luminance and three color differences) instead of three:

$$\begin{aligned} x_v &= \boldsymbol{v}^T\boldsymbol{x} \\ x_{d_i} &= x_i - s_i x_v = x_i - s_i \boldsymbol{v}^T\boldsymbol{x} \end{aligned} \tag{4}$$

One can easily check that the color difference vectors so defined are orthogonal to $\boldsymbol{s}$. The inverse projection is then

$$x_i = s_i x_v + x_{d_i} \tag{5}$$

Let $\hat{x}_i$ be a denoised version of x_i. From (5) it follows that the quality of estimate $\hat{x}_i = s_i\hat{x}_v + \hat{x}_{d_i}$ depends on $\boldsymbol{v}$ indirectly through the estimation error of $\hat{x}_v$ and $\hat{x}_{d_i}$. The constraint $\boldsymbol{v}^T\boldsymbol{s} = 1$ fixes the signal variance of x_v according to Lemma 1, and fixes the contribution of x_v in the inverse projection according to Lemma 2. The estimation error of color differences is comparatively small and can be neglected. Hence, choosing $\boldsymbol{v}$ that minimizes the variance of the luminance noise projection leads to optimal denoising. Lemma 3 relates optimal $\boldsymbol{v}$ to the signal and noise statistics.

Lemma 3 *Let $\boldsymbol{n} = (n_1, n_2, n_3)$ be the noise vector in RGB space and $\boldsymbol{\Sigma}_n$ its covariance matrix. Then the optimal vector $\boldsymbol{v}$ that yields the smallest projected noise variance is*

$$\boldsymbol{v}_{opt} = \arg \min_{\boldsymbol{v}^T\boldsymbol{s}=1} \boldsymbol{v}^T\boldsymbol{\Sigma}_n\boldsymbol{v} = \frac{\boldsymbol{\Sigma}_n^{-1}\boldsymbol{s}}{\boldsymbol{s}^T\boldsymbol{\Sigma}_n^{-1}\boldsymbol{s}} \tag{6}$$

Proof: Let $n_v = \boldsymbol{v}^T\boldsymbol{n}$ be the projection of $\boldsymbol{n}$ onto $\boldsymbol{v}$. The variance of n_v is $E\left\{n_v^T n_v\right\} = \boldsymbol{v}^T\boldsymbol{\Sigma}_n\boldsymbol{v}$. According to Lagrange multiplier method, the minimization of $\boldsymbol{v}^T\boldsymbol{\Sigma}_n\boldsymbol{v}$ under the constraint $\boldsymbol{v}^T\boldsymbol{s} = 1$ is equivalent to minimization of functional $\boldsymbol{v}^T\boldsymbol{\Sigma}_n\boldsymbol{v} - 2\lambda\boldsymbol{v}^T\boldsymbol{s}$, where 2λ is the Lagrange parameter. Setting the derivative of the functional to zero yields

$$\frac{d\left\{\boldsymbol{v}^T\boldsymbol{\Sigma}_n\boldsymbol{v} - 2\lambda\boldsymbol{v}^T\boldsymbol{s}\right\}}{d\boldsymbol{v}} = 2\boldsymbol{\Sigma}_n\boldsymbol{v} - 2\lambda\boldsymbol{s} = 0$$

Solving this equation for $\boldsymbol{v}$ and normalizing the result yields (6). ■

Fig. 3. Test images (Image 1 to Image 24, enumerated from left-to-right and top-to-bottom).

Table 3. CPSNR performance (in dB) by applying OCP in different approaches for grayscale images.

	Uniform noise			Nonuniform noise		
	Hard-Thr	Soft-Thr	GSM	Hard-Thr	Soft-Thr	GSM
RGB	27.03	27.59	27.80	26.95	27.48	27.72
YCbCr	28.30	28.77	28.90	27.84	28.31	28.46
OCP	28.73	29.21	29.72	29.35	29.75	30.44

4. EXPERIMENTAL RESULTS AND DISCUSSION

In our experiments we use 24 test color images shown in Fig. 3. Donoho's estimator [1] is adopted to compute the noise variance in each component σ_{n_i}, and then obtain the uncorrelated noise covariance matrix $\boldsymbol{\Sigma}_n$. The standard deviation of noise is estimated as

$$\hat{\sigma}_{n_i} = \frac{Median(|\tilde{x}_i|)}{0.6745} \tag{7}$$

where $\tilde{x}_i$ are the noisy HH wavelet coefficients. The signal vector is set as $\boldsymbol{s} = (1, 1, 1)^T$. As a performance measure we adopt the color peak signal-to-noise ratio (CPSNR), defined as the average Mean Square Error (MSE) of the denoised color components.

The proposed OCP can be combined with any grayscale wavelet-based denoising approach. In Table 3 we show the results of combining OCP with several existing approaches. Here, Hard-Thr and Soft-Thr are hard and soft thresholding of wavelet coefficients proposed in [4], and GSM stands for denoising based on Gaussian Scale Mixtures model, proposed by Portilla *et al.* [3]. We used redundant wavelet transform in Hard-Thr and Soft-Thr, and orthogonal wavelet transform in GSM. The proposed OCP outperforms RGB and YCbCr color spaces for all these methods.

We also compared the proposed OCP denoising with two recently proposed wavelet-based denoising methods, LSAI[2] [5] and MML [6][3]. The uHMT algorithm [2] is used in the proposed OCP denoising. For fairness, we adopt an orthogonal wavelet transform for all wavelet-based tested approaches. As shown in Table 4[4], the proposed approach outperforms all others on every test image.

OCP denoising approach performs especially well near the edges. To show this we partition the image into two regions corresponding to edges and smooth areas, and compare their denoising performance. We use Canny edge detection [14] followed by thresholding to obtain the classification. Table 5 shows the CPSNR of the

[2] We used the software provided by the authors with a minor modification to allow for different noise variances in the R, G and B components.

[3] The paper mentions two parameter estimation schemes: using MAP and ML framework. We adopted the latter because of better CPSNR.

[4] Due to limited space, we only present results for part of test images, but the average CPSNR is for all test images.

Table 4. CPSNR performance (in dB) of LSAI, MML, and the proposed OCP methods

Color Image	Uniform noise			Nonuniform noise		
	LSAI	MML	Ours	LSAI	MML	Ours
1	25.25	26.67	27.42	25.26	27.42	28.73
2	29.17	29.20	30.22	29.07	29.20	30.48
3	29.34	29.43	30.54	29.19	29.66	30.76
4	29.10	29.34	30.41	29.08	29.56	30.85
5	24.98	26.47	27.11	24.94	27.02	28.11
6	25.89	27.21	28.01	25.74	27.37	28.66
7	27.93	28.51	29.74	27.96	28.95	30.46
8	25.00	26.40	27.04	24.88	26.93	28.13
9	28.23	28.98	30.24	28.10	29.32	30.72
10	30.55	30.28	32.08	30.24	30.30	32.63
Average	27.47	28.18	29.18	27.36	28.44	29.81

Table 5. CPSNR performance (in dB) in the edge (E) and smooth (S) image regions.

Color Image		Uniform noise			Nonuniform noise		
		LSAI	MML	Ours	LSAI	MML	Ours
1	E	23.67	25.81	26.17	23.60	26.71	27.77
	S	27.37	27.59	28.93	27.54	28.15	29.81
2	E	26.61	27.69	28.28	26.55	27.88	28.86
	S	32.10	30.48	32.05	31.91	30.27	31.89
3	E	25.86	27.24	27.68	25.78	27.68	27.96
	S	32.76	30.92	32.86	32.46	30.95	32.98
4	E	26.63	27.88	28.47	26.66	28.32	29.09
	S	31.93	30.59	32.30	31.80	30.57	32.48
5	E	23.28	25.53	25.78	23.19	26.25	26.95
	S	27.38	27.51	28.75	27.45	27.84	29.47
Average	E	25.21	26.88	27.41	25.18	27.46	28.38
	S	30.34	29.51	31.25	30.13	29.55	31.51

two regions for LSAI, MML, and OCP methods. The proposed OCP denoising outperforms LSAI by 2-3 dB in edge regions and by 1-1.5 dB in smooth regions. MML denoising performs well in the edge region, but still about 0.5-0.9 dB worse compared to OCP. However, its performance in the smooth regions is quite poor, even when compared to the LSAI approach.

The visual quality improvements are even more striking than the PSNR gains. We applied the *wiener2*, LSAI, MML, and uHMT on OCP to test image, see Fig. 4. The OCP denoising preserves edges better than the other methods, while almost completely removing the color artifacts. MML also produces sharp edges, but fails in the smooth regions.

5. CONCLUSIONS

In this paper we developed a novel denoising approach that is based on similarity of detail wavelet coefficients across the color components. The denoising is done by projecting the image onto an optimal luminance/color-difference space adapted to image noise. The projection minimizes the noise in the luminance component, thus preserving the high-frequency contents of the image. On the other hand, the color-difference components are smooth and can be easily denoised despite the amount of the noise present.

Experimental results suggest that the proposed optimal color projection (OCP) approach outperforms the existing solutions both in PSNR and in visual quality. In particular, the OCP denoising demonstrates superior edge preservation properties while removing almost all color artifacts.


(a) Origin image


(b) Noisy image


(c) *wiener2*


(d) LSAI


(e) MML


(f) Ours

Fig. 4. Comparison of different denoising approaches on the Fence image corrupted by nonuniform noise.

6. REFERENCES

[1] D. L. Donoho and I. M. Johnstone, "Ideal spatial adaptation by wavelet shrinkage," *Biomitrika*, vol. 81, pp. 425-455, 1994.

[2] J. Romberg, H. Choi and R. G. Baraniuk, "Bayesian tree-structured image modeling using wavelet-domain hidden Markov models," *IEEE Trans. on Image Processing*, vol. 10, no. 7, pp. 1056-1068, July 2001.

[3] J. Portilla, V. Strela, M. J. Wainwright, and E. P. Simoncelli, "Image denoising using scale mixtures of

[4] M. Lang, H. Guo, J. E. Odegard, C. S. Burrus, and R. O. Wells, "Noise reduction using an undecimated discrete wavelet transform," *IEEE Signal Processing Letter*, vol. 3, pp. 10-12, Jan 1996.

[5] A. Pižurica and W. Philips, "Estimating probability of presence of a signal of interest in multiresolution single- and multiband image denoising," *to appear in IEEE Trans. on Image Processing*.

[6] P. Scheunders, J, Driesen,"Least-squares interband denoising of color and multispectral images," *IEEE Int. Conf. Image Processing*, Singapore, Oct 2004.

[7] O. Ben-Shahar and S. W. Zucher "Hue fields and color curvatures: a perceptual organization approach to color image denoising," *IEEE conference on CVPR*, June 2003.

[8] T. F. Chan, S. H. Kang, and J. Shen "Total variation denoising and enhancement of color images based on the CB and HSV color models," *Journal of Visual Communication and Image Representation*, vol. 12, pp. 422-435, June 2001.

[9] C. A. Poynton, "A technical introduction to digital video," John Wiley & Sons, Inc., 1996.

[10] B. Wandell, "Foundations of vision," Sinaur Associates, 1995.

[11] B. K. Gunturk, Y. Altunbasak and R. M. Mersereau, "Color plane interpolation using alternating projections," *IEEE Trans. on Image Processing*, vol. 11, no. 9, pp. 997-1013, Sep 2002.

[12] Y. Hel-Or, "The Canonical Correlations of Color Images and their use for Demosaicing," Technical Report, HP Labs, HPL-2003-164R1, Feb 2004.

[13] D. D. Muresan and T. P. Parks, "Demosaicking using optimal recovery," *IEEE Trans. on Image Processing*, vol. 14, no. 2, pp. 267-278, Feb 2005.

[14] J. F. Canny, "A computational approach to edge detection," *IEEE Trans. on Pattern Analysis and Machine Intelligence*, vol. 8, no. 6, pp. 679-698, Nov 1986.